Table 1 Continued

Patients	*NS223*	*NS231*	*NS239*	*NS248*	*NS254*	*NS263*	*NS299*	*NS318*	*NS324*	*Total*
Gender	F	F	M	M	F	M	F	F	F	
Age	6 months	5 months	18 years	5 years	2 months	1 month	3 years	1 month	1 year 6 months	
Paternal age at birth (years)	34	27	27	NA	37	35	34y	33	33	
Maternal age at birth (years)	36	27	26	30	34	36	35y	32	33	
Growth and development										
Postnatal failure to thrive	+	+	+	+	+	+	+	+	+	21/21
Mental retardation	+	+	+	+	NA	+	+	+	+	20/20
Craniofacial characteristics										
Relative macrocephaly	–	+	+	–	+	+	–	–	+	17/21
Coarse facial appearance	+	+	+	+	+	+	+	+	+	21/21
Muscloskeltal characteristics										
Short neck	–	+	NA	NA	+	+	+	–	–	14/19
Hyperextensive fingers	–	+	–	+	+	–	–	+	+	13/21
Tight Achilles tendon	+	NA	–	+	–	–	–	+	+	10/20
Abnormal foot position	–	–	NA	NA	NA	–	–	+	+	9/16
Skin characteristics										
Curly, sparse hair	+	Curly	Curly	+	+	+	Curly	+	Curly	21/21
Soft, loose skin	–	+	+	+	+	+	–	+	+	18/21
Deep palmer/planter creases	+	–	+	+	+	+	+	+	+	20/21
Cardiac defect										
Hypertrophic cardiomyopathy	+	–	+	+	+	+	+	+	+	14/20
Other	PAC	PVC	–	–	–	–	–	PAC	PAC	
Neoplasia										
Papillomata	+	–	+	–	–	–	–	–	–	6/20
Other tumors										
Others	Prabastatin administration	Laryngomalasia, hydrocephallus	GH deficiency, Arnold Chiari, scoliosis	Empty sella, GH deficiency, hypothyroidism, hypogonadism, syringomyelia		Hyperinsulinemia		Laryngomalasia seizure	Laryngomalasia	
HRAS mutation										
Nucleotide substitution	c.34G>T	c.35G>A	c.34G>A	c.34G>A	c.34G>A	c.35G>C	c.34G>A	c.35G>C	c.34G>A	
Amino acid substitution	p.G12C	p.G12D	p.G12S	p.G12S	p.G12S	p.G12A	p.G12S	p.G12A	p.G12S	

Abbreviations: –, absent; +, present; ASD, atrial septal defect; F, female; GER, gastroesophageal relfux; GH, growth hormone; GSDIII, glycogen storage disease III; M, male; NA, not available; PAC, premature atrial contraction; PS, pulmonic stenosis; PSVT, paroxysmal supraventricular tachycardia; PVC, premature ventricular contraction; VSD, ventricular septal defect.

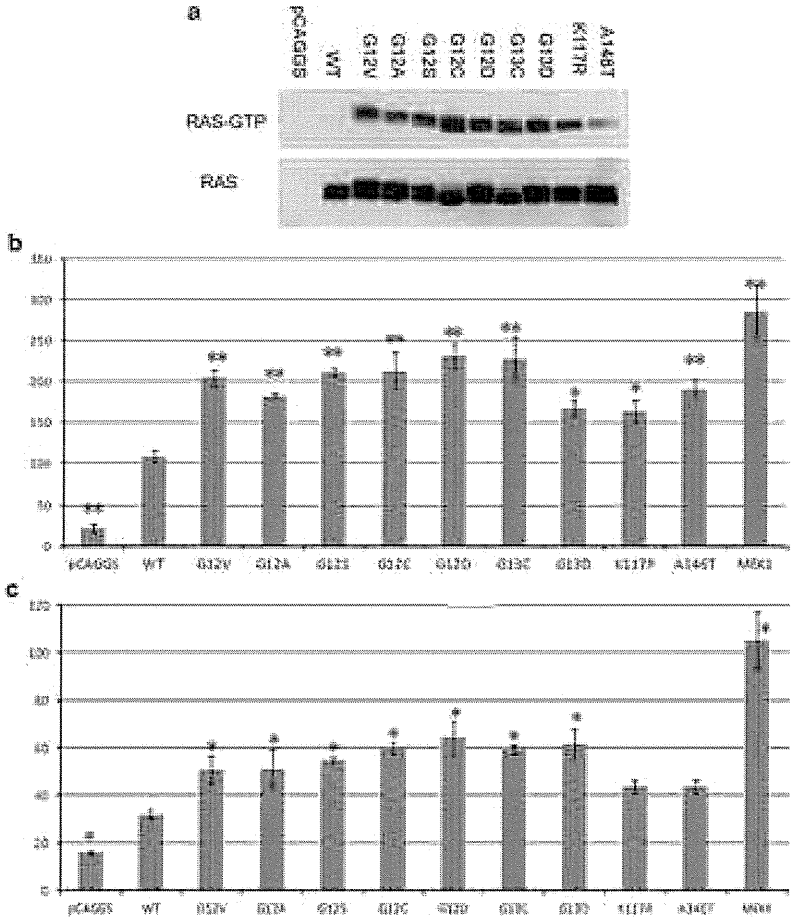

Figure 1 Functional characterization of HRAS mutants. (**a**) Ras-guanosine triphosphate (GTP) in NIH 3T3 cells transfected with wild-type or mutant HRAS constructs. HRAS protein levels were similar in NIH3T3 cells expressing each protein and were subsequently used as a loading control. (**b**, **c**) Stimulation of ELK (**b**) and c-Jun (**c**) transcription by *HRAS* mutants. The ELK-and c-Jun-GAL4 vectors and GAL4-luciferase trans-reporter vector were transiently co-transfected with various *HRAS* constructs into unstimulated NIH 3T3 cells. Relative luciferase activity (RLA) was normalized to the activity of a co-transfected control vector (phRLnull-luc) expressing *Renilla reniformis* luciferase. The results are expressed as the means and s.d. from triplicate samples. MEK1 and MEKK were used as positive controls. WT, wild type. $*P<0.05$; $**P<0.01$ compared with WT.

associated β-galactosidase staining confirmed that these cells showed cellular senescence.

Two downstream signaling pathways, p53 and Rb-p16, are activated during cellular senescence. To examine oncogene induced cellular senescence at the molecular level, we assessed senescence markers, including phosphorylated extracellular signal-regulated kinase, phosphorylated p53 and p16, in cells expressing HRAS mutant proteins (Figure 2b). As expected, phosphorylated p53 (Ser15) and p16 levels, as well as phospho-extracellular signal-regulated kinase levels, were significantly increased in the cells transfected with HRAS mutants relative to cells transfected with mock vector or wild-type HRAS. These results demonstrate that not only p.G12V, but also the other eight CS-related HRAS mutants, can cause OIS.

DISCUSSION

In this study, we identified four *HRAS* mutations in 21 patients with CS and evaluated their detailed clinical manifestations of the disease in these patients. Biochemical analyses, including a GTP binding assay and luciferase assays to detect ELK and c-Jun trans-activation, showed that there were no significant differences among the analyzed mutations in codon 12/13. The p.A146T mutant demonstrated the weakest Raf binding activity, and the p.K117R and p.A146T mutants had weaker effects on downstream c-Jun N-terminal kinase signaling than mutants in codon 12 or 13. Our results indicated that all HRAS mutants detected in CS patients were able to cause OIS.

Our study is the first to demonstrate that HRAS mutants other than p.G12V can induce senescence when they are overexpressed in human fibroblasts. The symptoms of CS seem to be caused by either hyperproliferation or hypoproliferation, coupled with growth factor resistance, which may be ascribable to DNA damage response or OIS. Postnatal cerebellar tonsillar herniation, Chiari 1 malformation,[42] deep palmar and plantar creases and papillomata may all be caused by hyperproliferation. In contrast, the poor weight gain, short stature and endocrine dysfunction observed in CS patients[43–45] might be caused by hypoproliferation. Adult brain and heart progenitor cells in a zebrafish CS model with a homozygous HRAS p.G12V mutation

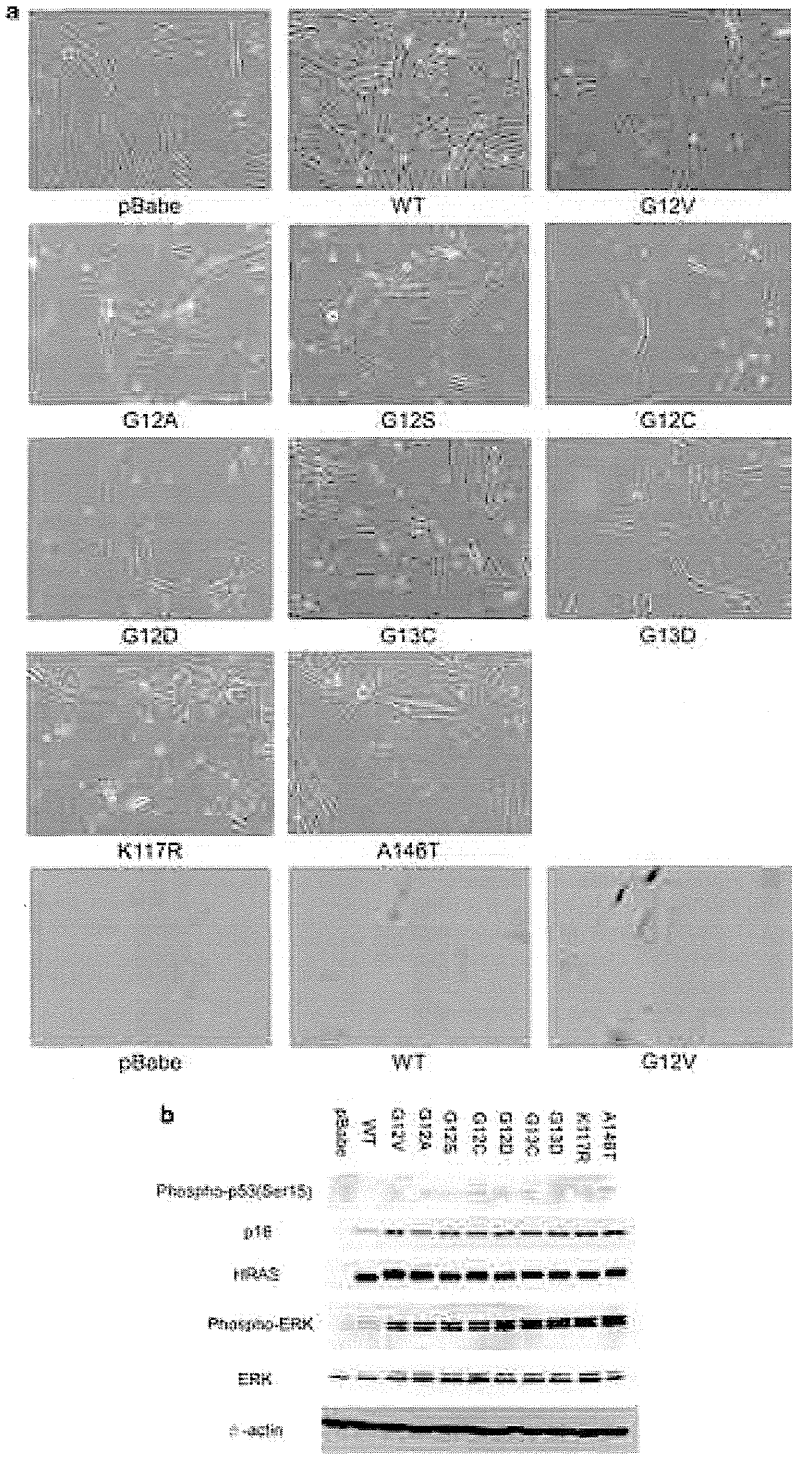

Figure 2 Effect of Costello syndrome (CS)-associated HRAS mutants on primary fibroblasts. (**a**) BJ cells transduced with retroviruses expressing wild-type or mutant HRAS. Images in the lowest tier show senescence-associated β-galactosidase staining. (**b**) Immunoblots of cellular lysates from BJ cells transduced with empty vector (pBabe) or with wild-type or mutant HRAS retroviruses.

exhibited cellular senescence, suggesting that the age-related worsening of the Costello phenotype[46] might occur, because the replicative capability of adult progenitor cells is exhausted. Osteoporosis has frequently been found in adult patients with CS,[47] suggesting that cellular senescence affects osteogenesis. However, further studies will be needed to determine whether OIS indeed contributes to the pathogenesis in patients with CS.

It has been suggested that clinical symptoms vary among patients with mutations in codon 12 or 13. In previous studies, a total of 19 CS patients have been reported to die from severe cardiomyopathy, cardiac arrhysmia, rhabdomyosarcoma, respiratory failure, multi-organ failure or sepsis. The number of fatal cases was 5/138 patients with p.G12S, 4/6 with p.G12C, 3/17 with p.G12A, 3/4 with p.G12D, 2/2 with p.G12V, 1/1 with p.G12E and 1/1 with p.E63K.[3,5–23] The mortality of patients with p.G12C or p.G12D was significantly higher than that of the patients with the more common p.G12S (P=0.026 by Fisher's exact test). Previous studies have shown that the p.G12V substitution has the highest transformative potential (p.G12V > p.G12A, p.G12S, p.G12C, p.G12D > p.G13D) and is the most frequently found mutation in human tumors.[48,49] However, our Ras activity assays and luciferase assays did not show any differences among *HRAS* codon 12/13 mutants. This may be due to the extremely high expression level of HRAS protein in our transient transfection study, which could make it difficult to detect subtle differences between mutants. Further studies will be necessary to clarify whether the high mortality in patients with p.G12C or p.G12D is due to functional differences in these mutants or due to bias because of our small sample size of patients.

Mutations at codons 117 and 146 are rare in CS and somatic cancers. Meanwhile, mutations at codons G12, G13 and Q61 have been shown to impair intrinsic and GTPase activating protein-mediated GTP hydrolysis, leading to elevated levels of cellular RAS-GTP. It has been reported that the nucleotide exchange rate of both p.K117R and p.A146V HRAS is increased, relative to wild type.[13,27,28] However, the transformational potential of p.A146V HRAS is partially activated,[27] whereas that of p.K117R-HRAS is not; its transformational activity is instead similar to that of GTPase impaired mutants.[28] Our results and those of other reports suggest that p.K117R and p.A146T have milder effects on downstream effectors than do mutations in codon 12/13.

The clinical manifestations of CS in patients with p.K117R or p.A146V mutations suggest that these alleles have distinct effects, compared with mutations in codon 12/13. Of two CS patients with a p.K117R mutation, one patient had an atypical phenotype such as microretrognatism and slightly less-pronounced plantar and palmar creases.[7] The other patient had mild craniofacial manifestations of CS.[13] One patient with the p.A146V mutation showed a mildly coarse face and did not have deep palmar creases.[6] These atypical phenotypes might be attributed to the mild effects of p.K117R or p.A146V compared with codon 12/13 mutants.

Inhibitors of the RAS/MAPK pathway could provide benefits for patients with RAS/MAPK syndromes. Statins are 3-hydroxy-3-methyl-glutaryl-CoA reductase inhibitors that result in decreased isoprenylation of RAS[50] and are now widely used for the treatment of hyperlipidemia. Statins have been used to modify the clinical manifestation of neurofibromatosis type I, which is caused by a genetic defect in a negative regulator of the RAS/MAPK pathway. Studies using mouse models of NF1 (Nf1 mice) have shown that treatment with a statin reverses the cognitive deficits of these mice.[51] A randomized control trial for neurofibromatosis type I treatment with simvastatin had a negative outcome.[52] Furthermore, statins have displayed antitumor activity in experimental tumor models, though clinical antitumor effects of statins have not been established.[53] Well-designed clinical studies will be needed to determine the effects of statins or other RAS inhibitors on manifestations of CS.

In conclusion, we identified *HRAS* mutations in 21 patients and examined the clinical manifestations of mutation-positive patients. Functional analysis revealed that CS-causing mutant HRAS proteins caused OIS in human fibroblasts. These findings may help enable more accurate prognoses for patients with *HRAS* mutations and contribute to our understanding of the mechanism underlying CS pathogenesis.

CONFLICT OF INTEREST

The authors declare no conflict of interest.

ACKNOWLEDGEMENTS

We thank the patients who participated in this study and their families and doctors, including Naoki Watanabe and Tomohiro Iwasaki, who referred the cases. We are grateful to Dr Garry Nolan of Stanford University for supplying Phoenix-Eco and Ampho cells, to Dr William C Hahn for supplying the pBabe-zeo-ecotropic receptor vector, and to Dr Jun-ichi Miyazaki of Osaka University for supplying the pCAGGS expression vector. We are also grateful to Drs Noriko Ishida and Keiko Nakayama for their technical assistance with the infection of retroviral vectors. We thank Kumi Kato and Hasumi Haba for their technical assistance. This work was supported by Grants-in-Aids for young scientists (A and S) from the Ministry of Education, Culture, Sports, Science and Technology of Japan (nos. 19689022, 21689029 and 19679005) to TN and YA, the Science and Technology Foundation of Japan Grant-in-Aid for Scientific Research to TN, and the Ministry of Health, Labour and Welfare to YM and YA.

1 Hennekam, R. C. Costello syndrome: an overview. *Am. J. Med. Genet. C. Semin. Med. Genet.* **117C,** 42–48 (2003).
2 Aoki, Y., Niihori, T., Narumi, Y., Kure, S. & Matsubara, Y. The RAS/MAPK syndromes: novel roles of the RAS pathway in human genetic disorders. *Hum. Mutat.* **29,** 992–1006 (2008).
3 Aoki, Y., Niihori, T., Kawame, H., Kurosawa, K., Ohashi, H., Tanakam, Y. *et al.* Germline mutations in HRAS proto-oncogene cause Costello syndrome. *Nat. Genet.* **37,** 1038–1040 (2005).
4 Kerr, B., Allanson, J., Delrue, M. A., Gripp, K. W., Lacombe, D., Lin, A. E. *et al.* The diagnosis of Costello syndrome: nomenclature in Ras/MAPK pathway disorders. *Am. J. Med. Genet. A* **146A,** 1218–1220 (2008).
5 Estep, A. L., Tidyman, W. E., Teitell, M. A., Cotter, P. D. & Rauen, K. A. HRAS mutations in Costello syndrome: detection of constitutional activating mutations in codon 12 and 13 and loss of wild-type allele in malignancy. *Am. J. Med. Genet. A.* **140,** 8–16 (2006).
6 Gripp, K. W., Lin, A. E., Stabley, D. L., Nicholson, L., Scott, C. I. Jr, Doyle, D. *et al.* HRAS mutation analysis in Costello syndrome: genotype and phenotype correlation. *Am. J. Med. Genet. A.* **140,** 1–7 (2006).
7 Kerr, B., Delrue, M. A., Sigaudy, S., Perveen, R., Marche, M., Burgelin, I. *et al.* Genotype-phenotype correlation in Costello syndrome: HRAS mutation analysis in 43 cases. *J. Med. Genet.* **43,** 401–405 (2006).
8 van Steensel, M. A., Vreeburg, M., Peels, C., van Ravenswaaij-Arts, C. M., Bijlsma, E., Schrander-Stumpel, C. T. *et al.* Recurring HRAS mutation G12S in Dutch patients with Costello syndrome. *Exp. Dermatol.* **15,** 731–734 (2006).
9 Gripp, K. W., Lin, A. E., Nicholson, L., Allen, W., Cramer, A., Jones, K. L. *et al.* Further delineation of the phenotype resulting from BRAF or MEK1 germline mutations helps differentiate cardio-facio-cutaneous syndrome from Costello syndrome. *Am. J. Med. Genet. A.* **143A,** 1472–1480 (2007).
10 Orstavik, K. H., Tangeraas, T., Molven, A. & Prescott, T. E. Distal phalangeal creases—a distinctive dysmorphic feature in disorders of the RAS signalling pathway? *Eur. J. Med. Genet.* **50,** 155–158 (2007).
11 Sovik, O., Schubbert, S., Houge, G., Steine, S. J., Norgard, G., Engelsen, B. *et al. De novo* HRAS and KRAS mutations in two siblings with short stature and neuro-cardio-facio-cutaneous features. *J. Med. Genet.* **44,** e84 (2007).
12 Zampino, G., Pantaleoni, F., Carta, C., Cobellis, G., Vasta, I., Neri, C. *et al.* Diversity parental germline origin, and phenotypic spectrum of *de novo* HRAS missense changes in Costello syndrome. *Hum. Mutat.* **28,** 265–272 (2007).
13 Denayer, E., Parret, A., Chmara, M., Schubbert, S., Vogels, A., Devriendt, K. *et al.* Mutation analysis in Costello syndrome: functional and structural characterization of the HRAS pLys117Arg mutation. *Hum. Mutat.* **29,** 232–239 (2008).

14 Gripp, K. W., Innes, A. M., Axelrad, M. E., Gillan, T. L., Parboosingh, J. S., Davies, C. *et al.* Costello syndrome associated with novel germline HRAS mutations: an attenuated phenotype? *Am. J. Med. Genet. A.* **146A,** 683–690 (2008).
15 Hou, J. W. Rapidly progressive scoliosis after successful treatment for osteopenia in Costello syndrome. *Am. J. Med. Genet. A.* **146,** 393–396 (2008).
16 Limongelli, G., Pacileo, G., Digilio, M. C., Calabro, P., Di Salvo, G., Rea, A. *et al.* Severe, obstructive biventricular hypertrophy in a patient with Costello syndrome: clinical impact and management. *Int. J. Cardiol.* **130,** e108–e110 (2008).
17 Schulz, A.L., Albrecht, B., Arici, C., van der Burgt, I., Buske, A., Gillessen-Kaesbach, G. *et al.* Mutation and phenotypic spectrum in patients with cardio-facio-cutaneous and Costello syndrome. *Clin. Genet.* **73,** 62–70 (2008).
18 Gremer, L., De Luca, A., Merbitz-Zahradnik, T., Dallapiccola, B., Morlot, S., Tartaglia, M. *et al.* Duplication of Glu37 in the switch I region of HRAS impairs effector/GAP binding and underlies Costello syndrome by promoting enhanced growth factor-dependent MAPK and AKT activation. *Hum. Mol. Genet.* **19,** 790–802 (2010).
19 Kuniba, H., Pooh, R.K., Sasaki, K., Shimokawa, O., Harada, N., Kondoh, T. *et al.* Prenatal diagnosis of Costello syndrome using 3D ultrasonography amniocentesis confirmation of the rare HRAS mutation G12D. *Am. J. Med. Genet. A.* **149A,** 785–787 (2009).
20 Lin, A. E., O'Brien, B., Demmer, L. A., Almeda, K. K., Blanco, C. L., Glasow, P. F. *et al.* Prenatal features of Costello syndrome: ultrasonographic findings and atrial tachycardia. *Prenat. Diagn.* **29,** 682–690 (2009).
21 Piccione, M., Piro, E., Pomponi, M. G., Matina, F., Pietrobono, R., Candela, E. *et al.* A premature infant with Costello syndrome due to a rare G13C HRAS mutation. *Am. J. Med. Genet. A.* **149A,** 487–489 (2009).
22 Sol-Church, K., Stabley, D. L., Demmer, L. A., Agbulos, A., Lin, A. E., Smoot, L. *et al.* Male-to-male transmission of Costello syndrome: G12S HRAS germline mutation inherited from a father with somatic mosaicism. *Am. J. Med. Genet. A.* **149A,** 315–321 (2009).
23 Zhang, H., Ye, J. & Gu, X. Recurring G12S mutation of HRAS in a Chinese child with Costello syndrome with high alkaline phosphatase level. *Biochem. Genet.* **47,** 868–871 (2009).
24 van der Burgt, I., Kupsky, W., Stassou, S., Nadroo, A., Barroso, C., Diem, A. *et al.* Myopathy caused by HRAS germline mutations: implications for disturbed myogenic differentiation in the presence of constitutive HRas activation. *J. Med. Genet.* **44,** 459–462 (2007).
25 McGrath, J. P., Capon, D. J., Goeddel, D. V. & Levinson, A. D. Comparative biochemical properties of normal and activated human ras p21 protein. *Nature.* **310,** 644–649 (1984).
26 Al-Mulla, F., Milner-White, E. J., Going, J. J. & Birnie, G. D. Structural differences between valine-12 and aspartate-12 Ras proteins may modify carcinoma aggression. *J. Pathol.* **187,** 433–438 (1999).
27 Feig, L. A. & Cooper, G. M. Relationship among guanine nucleotide exchange, GTP hydrolysis, and transforming potential of mutated ras proteins. *Mol. Cell. Biol.* **8,** 2472–2478 (1988).
28 Der, C. J., Weissman, B. & Macdonald, M. J. Altered guanine-nucleotide binding and H-Ras transforming and differentiating activities. *Oncogene.* **3,** 105–112 (1988).
29 Sikora, E., Arendt, T., Bennett, M. & Narita, M. Impact of cellular senescence signature on ageing research. *Ageing Res. Rev.* **10,** 146–152 (2010).
30 Serrano, M., Lin, A. W., McCurrach, M. E., Beach, D. & Lowe, S. W. Oncogenic ras provokes premature cell senescence associated with accumulation of p53 and p16INK4a. *Cell* **88,** 593–602 (1997).
31 Narita, M., Nunez, S., Heard, E., Narita, M., Lin, A. W., Hearn, S. A. *et al.* Rb-mediated heterochromatin formation and silencing of E2F target genes during cellular senescence. *Cell* **113,** 703–716 (2003).
32 Di Micco, R., Fumagalli, M., Cicalese, A., Piccinin, S., Gasparini, P., Luise, C. *et al.* Oncogene-induced senescence is a DNA damage response triggered by DNA hyper-replication. *Nature* **444,** 638–642 (2006).
33 Bartkova, J., Rezaei, N., Liontos, M., Karakaidos, P., Kletsas, D., Issaeva, N. *et al.* Oncogene-induced senescence is part of the tumorigenesis barrier imposed by DNA damage checkpoints. *Nature* **444,** 633–637 (2006).
34 Narita, M. & Lowe, S. W. Senescence comes of age. *Nat. Med.* **11,** 920–922 (2005).
35 Campisi, J. Suppressing cancer: the importance of being senescent. *Science* **309,** 886–887 (2005).
36 Kawame, H., Matsui, M., Kurosawa, K., Matsuo, M., Masuno, M., Ohashi, H. *et al.* Further delineation of the behavioral and neurologic features in Costello syndrome. *Am. J. Med. Genet. A.* **118A,** 8–14 (2003).
37 Kalfa, D., Fraisse, A. & Kreitmann, B. Medical and surgical perspectives of cardiac hypertrophy in Costello syndrome. *Cardiol. Young* **19,** 644–647 (2009).
38 Digilio, M. C., Sarkozy, A., Capolino, R., Chiarini Testa, M. B., Esposito, G., de Zorzi, A. *et al.* Costello syndrome: clinical diagnosis in the first year of life. *Eur. J. Pediatr.* **167,** 621–628 (2008).
39 Schuhmacher, A. J., Guerra, C., Sauzeau, V., Canamero, M., Bustelo, X. R. & Barbacid, M. A mouse model for Costello syndrome reveals an Ang II-mediated hypertensive condition. *J. Clin. Invest.* **118,** 2169–2179 (2008).
40 Kaji, M., Kurokawa, K., Hasegawa, T., Oguro, K., Saito, A., Fukuda, T. *et al.* A case of Costello syndrome and glycogen storage disease type III. *J. Med. Genet.* **39,** E8 (2002).
41 Omori, I., Shimizu, M. & Watanabe, T. An infant with Costello syndrome and a rare HRAS mutation (G12C). *J. Jpn. Pediatr. Soc.* **114,** 1592–1597 (2010).
42 Gripp, K. W., Hopkins, E., Doyle, D. & Dobyns, W.B. High incidence of progressive postnatal cerebellar enlargement in Costello syndrome: brain overgrowth associated with HRAS mutations as the likely cause of structural brain and spinal cord abnormalities. *Am. J. Med. Genet. A.* **152A,** 1161–1168 (2010).
43 Gregersen, N. & Viljoen, D. Costello syndrome with growth hormone deficiency and hypoglycemia: a new report and review of the endocrine associations. *Am. J. Med. Genet. A.* **129A,** 171–175 (2004).
44 Stein, R. I., Legault, L., Daneman, D., Weksberg, R. & Hamilton, J. Growth hormone deficiency in Costello syndrome. *Am. J. Med. Genet. A.* **129A,** 166–170 (2004).
45 Alexander, S., Ramadan, D., Alkhayyat, H., Al-Sharkawi, I., Backer, K. C., El-Sabban, F. *et al.* Costello syndrome and hyperinsulinemic hypoglycemia. *Am. J. Med. Genet. A.* **139,** 227–230 (2005).
46 Santoriello, C., Deflorian, G., Pezzimenti, F., Kawakami, K., Lanfrancone, L., d'Adda di Fagagna, F. *et al.* Expression of H-RASV12 in a zebrafish model of Costello syndrome causes cellular senescence in adult proliferating cells. *Dis. Model. Mech.* **2,** 56–67 (2009).
47 White, S. M., Graham, J. M. Jr, Kerr, B., Gripp, K., Weksberg, R., Cytrynbaum, C. *et al.* The adult phenotype in Costello syndrome. *Am. J. Med. Genet. A.* **136,** 128–135 (2005).
48 Seeburg, P. H., Colby, W. W., Capon, D. J., Goeddel, D. V. & Levinson, A. D. Biological properties of human c-Ha-ras1 genes mutated at codon 12. *Nature* **312,** 71–75 (1984).
49 Fasano, O., Aldrich, T., Tamanoi, F., Taparowsky, E., Furth, M. & Wigler, M. Analysis of the transforming potential of the human H-ras gene by random mutagenesis. *Proc. Natl Acad. Sci. USA* **81,** 4008–4012 (1984).
50 Jakobisiak, M. & Golab, J. Statins can modulate effectiveness of antitumor therapeutic modalities. *Med. Res. Rev.* **30,** 102–135 (2010).
51 Li, W., Cui, Y., Kushner, S. A., Brown, R. A., Jentsch, J. D., Frankland, P. W. *et al.* The HMG-CoA reductase inhibitor lovastatin reverses the learning and attention deficits in a mouse model of neurofibromatosis type 1. *Curr. Biol.* **15,** 1961–1967 (2005).
52 Krab, L. C., de Goede-Bolder, A., Aarsen, F. K., Pluijm, S. M., Bouman, M. J., van der Geest, J. N. *et al.* Effect of simvastatin on cognitive functioning in children with neurofibromatosis type 1: a randomized controlled trial. *JAMA* **300,** 287–294 (2008).
53 Dale, K. M., Coleman, C. I., Henyan, N. N., Kluger, J. & Whitem, C. M. Statins and cancer risk: a meta-analysis. *JAMA* **295,** 74–80 (2006).

Congenital Anomalies
THE JAPANESE TERATOLOGY SOCIETY
doi:10.1111/cga.12004
Congenital Anomalies 2013; **53**, 67–72

ORIGINAL ARTICLE

Craniofacial and dental malformations in Costello syndrome: A detailed evaluation using multi-detector row computed tomography

Masashi Takahashi[1] and Hirofumi Ohashi[2]
[1]Department of Pediatric Dentistry, Nihon University Graduate School of Dentistry at Matsudo, Matsudo, and [2]Division of Medical Genetics, Saitama Children's Medical Center, Saitama, Japan

ABSTRACT **Costello syndrome is a rare multiple congenital anomaly syndrome caused by heterozygous germline *HRAS* mutations, which is characterized by intellectual disability, growth retardation, distinctive facies, loose skin, cardiomyopathy and a preposition to malignancies. Although teeth abnormalities have been encountered in nearly two-thirds of the patients in literature, the evaluation tended to be limited to the extent which can be obtained from physical examination. We investigated detailed craniofacial, oral and dental findings in four patients with Costello syndrome. In this study, images reconstructed by multi-detector row computed tomography (MDCT) were used as substitutes for dental cast study and panoramic and lateral cephalometric radiograph studies to evaluate dental arches, tooth size, relationships between craniofacial and dental structures, and hypodontia. All four patients showed true/relative macrocephaly with facial bone hypoplasia and gingival hypertrophy. Occlusal attrition, malocclusion, small dental arches, microdontia, and convex face were noted in three patients. In addition, one patient showed dental caries, conic tooth and gingivitis, and another patient showed hypodontia. Our study suggests that craniofacial and dental abnormalities are common in Costello syndrome patients and comprehensive dental care should be provided from early infancy. To our knowledge, this is the first study of thorough craniofacial and dental evaluation by using MDCT in Costello syndrome. MDCT is a useful tool for precise evaluation of craniofacial and oral manifestations in patients with congenital anomaly/intellectual disability syndromes.**

Key Words: cephalometric analysis, Costello syndrome, multi-detector row computed tomography, small dental arch, malocclusion

INTRODUCTION

Costello syndrome is a rare multiple congenital anomaly syndrome characterized by intellectual disability, growth retardation, distinctive facies, loose skin, cardiomyopathy and a preposition to malignancies (Hennekam 2003), the prevalence of which is estimated to be 1 in 1 290 000 (Abe et al. 2012). Costello syndrome is caused by heterozygous germline *HRAS* mutations (Aoki et al. 2005) and is listed as one of the RASopathies, a group of related disorders caused by germline mutations in the Ras/mitogen-activated protein kinase pathway, which includes Noonan syndrome, cardio-facio-cutaneous (CFC) syndrome, and Costello syndrome, with considerable phenotypic overlap among these disorders (Rauen et al. 2010).

Craniofacial and oral features previously reported in Costello syndrome include macrocephaly, prominent forehead, high-arched palate, macroglossia, gingival hypertrophy, malocclusion, enamel hypoplasia and caries (Der Kaloustian et al. 1991; Di Rocco et al. 1993; Teebi and Shaabani 1993; Zampino et al. 1993; Johnson et al. 1998; van Eeghen et al. 1999; Delrue et al. 2003; Hennekam 2003; Kawame et al. 2003). Although teeth abnormalities were encountered in nearly two-thirds of the patients in the comprehensive review by Hennekam et al. (2003), the evaluation tended to be limited to the extent that can be obtained from physical examination. We here report on the result of our investigation of detailed craniofacial, oral and dental findings in four patients with Costello syndrome by using multi-detector row computed tomography (MDCT).

MATERIALS AND METHODS

Patients

A total of four patients with Costello syndrome, two male and two female, ranging in age between 5 and 7 years, were included in this study. All four patients were identified as having a missense mutation in the *HRAS* gene; c.34G>A (p.Gly12Ser) in patients 1, 2 and 3, and c.38G>A (p.Gly13Asp) in patient 4, either in exon 2. Clinical manifestations of the four patients are shown in Table 1. This study protocol was approved by the Ethics Committee of Saitama Children's Medical Center and proper informed consent was obtained from the legal guardians of patients.

Oral, dental, and craniofacial studies

Intraoral features such as palatal morphology, tooth calcification, occlusion and tooth eruption status were evaluated on physical examination. In addition, images reconstructed by MDCT were used as substitutes for dental cast study and panoramic and lateral cephalometric radiograph studies to evaluate the dental arches, tooth size, relationships between craniofacial and dental structures, and hypodontia. The following MDCT imaging conditions were used: window width, 1500; and window level, 450 (Hirai et al. 2010, 2011; Yamauchi et al. 2010). Crown and dental arch sizes were measured using Image J with a resolution accuracy of 0.1 mm. Lateral cephalometric analysis was performed based on the method developed by Iizuka and Ishikawa (1957). To perform cephalometric measurements, we made adjustments by rotating the mandibular bone image toward the expected actual intercuspal position. All measured data in this study were compared with standard values for

Correspondence: Masashi Takahashi, Department of Pediatric Dentistry, Nihon University Graduate School of Dentistry at Matsudo, 2-870-1 Sakaecho-Nishi, Matsudo, Chiba 271-8587, Japan. Email: matakahashidentist@yahoo.co.jp
Received September 24, 2012; revised and accepted November 4, 2012.

Table 1 Clinical manifestations of four patients with Costello syndrome

Patients	1	2	3	4
Gender	M	M	F	F
Age (years)	5	6	6	7
Intellectual disability	+ (Severe)	+	+	+
Height (SD)	−6.8	−5.9	−4.9	−2.7
Head circumference (SD)	−2.5	+0.27	+0.29	+2.9
Distinctive facies	+	+	+	+
Cardiac defect	HCM, AT	HCM, AT, VSD, MR	−	HCM, AT
Skeletal abnormality	HD, FD	HD, FD	HD, FD	FD
Neoplasia	−	−	−	−
Other	Tracheomalacia	Inguinal hernia	Exotropia	GHD
HRAS mutation	c.34G>A (p.G12S)	c.34G>A (p.G12S)	c.34G>A (p.G12S)	c.38G>A (p.13G>D)

+, present; −, absent; AT, atrial tachycardia; F, female; FD, foot deformity; GHD, growth hormone deficiency; HCM, hypertrophic cardiomyopathy; HD, hip dislocation; M, male; MR, mitral regurgitation; VSD, ventricular septal defect.

Japanese individuals (Iizuka and Ishikawa 1957; Otsubo 1964; Kato 1979; Fukawa 2008).

RESULTS

Oral and dental features noted in four patients are summarized in Table 2. On physical examination, all four patients had open mouth, thick lips and gingival hypertrophy. Other common features noted in all but one patient were occlusal attrition (patients 1, 2, 3), high-arched palate (patients 2,3,4) and malocclusion (patients 1 and 4 exhibited open bite, and patient 3 cross bite). In addition, one patient (patient 4) exhibited dental caries in a single tooth, a single conic tooth, and gingivitis. Enamel hypoplasia, an occasionally reported feature in patients with Costello syndrome, was not apparent in any of our patients (Fig. 1). Crowding of teeth was also not observed in the four patients. Panolamic images reconstructed with MDCT revealed a congenital tooth defect (mandibular left second premolar) in one patient (patient 3; Fig. 2).

Small dental arch was present in all patients except patient 1 (Table 3). Morphological categorization of small dental arches in the three patients were as follows: one patient (patient 2) exhibited U-shaped dental arch in the maxilla and narrow dental arch in the mandible; and two patients (patients 3 and 4) showed narrow dental arch in the maxilla and rectangular dental arch in the mandible (Fig. 3).

In terms of tooth size, maxillary teeth, especially lateral incisors and first and second molars in primary teeth and first molar in permanent teeth, tend to be small in these patients studied (Table 4). The degree of smallness of the maxillary teeth was most marked in the second molars in primary teeth of the two male patients (patients 1 and 2).

Cephalometric analysis (Table 5) revealed that, among the four patients studied, a convex face (increased facial convexity) was present in three patients (patients 1, 2 and 3), associated with maxillary overhang (increased SNA angle) observed in one patient (Patient 1), and with mandibular retrusion (decreased SNB angle) in two patients (patients 2 and 3).

Three-dimensional reconstructed images by MDCT also demonstrated the craniofacial manifestations shared by all four patients such as true/relative macrocephaly with maxillofacial hypoplasia, dolichocephaly, and mandibular anomalies characterized by thick and flat head of the condylar process, short condylar neck, narrow mandibular notch, and antegonial notching (Fig. 4). Calcified falx cerebri were also noted in all patients.

Table 2 Oral and dental features in four patients with Costello syndrome

	Patient				
	1	2	3	4	Total
Open mouth	+	+	+	+	4/4
Thick lips	+	+	+	+	4/4
Gingival hypertrophy	+	+	+	+	4/4
Gingivitis	−	−	−	+	1/4
Dental caries	−	−	−	+	1/4
Occlusal attrition	+	+	+	−	3/4
Relative macrocephaly with facial bone hypoplasia	+	+	+	+	4/4
High-arched palate	−	+	+	+	3/4
Convex face	+	+	+	−	3/4
Maxillary overhang	+	−	−	−	1/4
Mandibular retrusion	−	+	+	−	2/4
Malocclusion	O	−	C	O	3/4
Small dental arch	−	+	+	+	3/4
Maxilla	U	U	N	N	
Mandible	U	N	R	R	
Hypodontia	−	−	+	−	1/4
Conic teeth	−	−	−	+	1/4

+, present; −, absent; C, cross bite; O, open bite; N, narrow dental arch; R, rectangle dental arch; U, U-shaped dental arch.

DISCUSSION

We performed thorough evaluation of craniofacial and dental features in four patients with Costello syndrome. As previously

Table 3 Dental arch measurements in four patients

Patient	1		2		3		4	
	L1	L2	L1	L2	L1	L2	L1	L2
Maxilla	1.25	−0.67	−2.06	−2.90	−1.61	−2.52	−0.91	−1.04
Mandibular	0.79	−0.38	2.50	−0.06	−3.30	−1.98	−3.86	−2.42
	WC	WE	WC	WE	WC	WE	WC	WE
Maxilla	0.97	−0.02	−1.31	−2.88	−4.14	−2.80	−1.45	−1.52
Mandibular	0.97	0.51	−2.98	−1.49	−1.66	−0.24	−3.02	−2.53

WC and WE represent the distance between the primary cuspids (the cuspids), and the primary second molars, respectively. L1 represents the distance between the central point of the incisors and the line connecting the primary cuspids of both sides, and L2 represents the distance between the central point of the incisors and the line connecting the primary second molars of both sides. Unit, S.D.

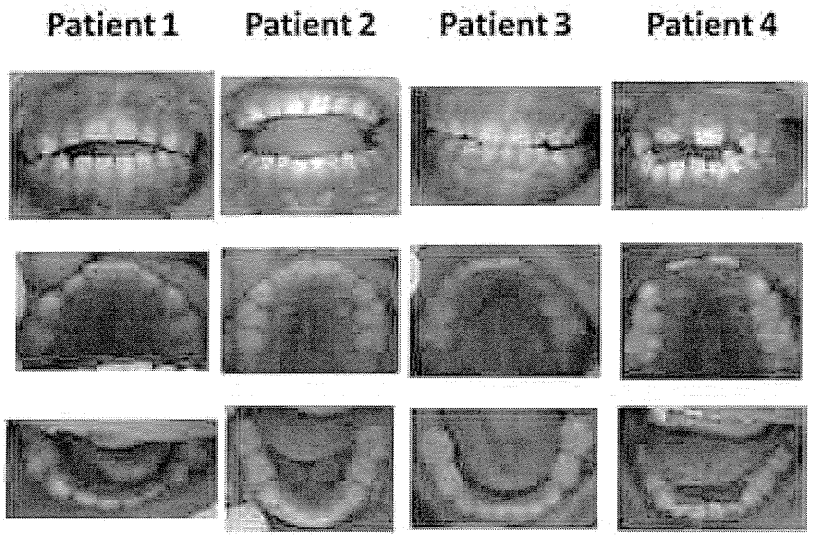

Fig. 1 Oral photographs of four patients. Patients 2, 3 and 4 showed occlusal attrition, high-arched palate and small dental arch. Patient 4 showed dental caries, gingivitis and conic teeth.

Fig. 2 Multi-detector row computed tomography (MDCT)-synthesized panoramic radiograph of Patient 3 at 6 years of age. Note the missing lower second premolar on left side (arrow).

reported, our patients showed true/relative macrocephaly and gingival hypertrophy (all patients). In addition, they exhibited malocclusion, occlusal attrition, small dental arches, microdontia, and convex face (three patients). Dental caries, conic tooth and gingivitis were noted in one patient, and hypodontia was noted in another patient. Enamel hypoplasia, an occasionally reported feature in patients with Costello syndrome, was not apparent in any of our patients.

True/relative macrocephaly is a well-known feature of patients with Costello syndrome. In this study, MDCT images showed macrocephalic skull in all four patients. In addition, facial bone hypoplasia was also evident which was associated with malformed mandible characterized by thick and flat head of the condylar process, short condylar neck, narrow mandibular notch, and antegonial notching on MDCT (Fig. 4). Antegonial notching is a feature seen in several congenital malformation syndromes associated with facial bone dysplasia, such as Treacher Collins syndrome, Nager syndrome and Pierre-Robin syndrome (Becker et al. 1976). Facial skeletal maldevelopment should be considered a feature of Costello syndrome.

Occlusal attrition is a finding that was frequently observed in our patients (patients 2, 3, 4). While the causes of attrition are diverse, malocclusion and habits such as bruxism and clenching are main possible causes. In view of behavioral characteristics of irritability of patients with Costello syndrome, habits such as teeth clenching might be a major cause for attrition.

It is of interest to know whether there are phenotypic similarities in craniofacial and dental features among Noonan-related disorders

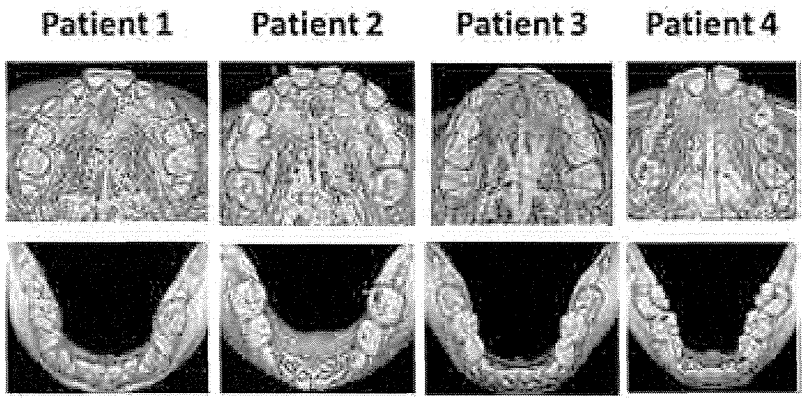

Fig. 3 Multi-detector row computed tomography (MDCT)-synthesized upper and lower dental arches in all four patients. Small dental arches are noted in three patients (patients 2, 3 and 4). Patient 2 exhibited a U-shaped dental arch in the maxilla and narrow dental arch in the mandible; Patients 3 and 4 exhibited narrow dental arches in the maxilla and rectangle arches in the mandible.

Table 4 Tooth size measurements in four patients

Patient	1		2		3		4	
	Right	Left	Right	Left	Right	Left	Right	Left
Maxillary								
Primary teeth								
Central incisor	0.54	0.54	−1.08	−0.54	−0.45	−0.45		
Lateral incisor	−2.00	−1.78	−1.56	−1.56	−2.44	−2.44	−0.49	
Cuspid	−1.22	−0.98	−1.22	−1.71	−0.73	−0.73	−0.98	−0.24
First molar	−2.39	−2.61	−2.17	−1.96	−1.09	−0.87	−0.43	−0.43
Second molar	−3.33	−3.16	−3.68	−3.51	−1.93	−1.58	−1.05	−0.53
Permanent teeth								
Central incisor							0.24	0.98
First molar							−1.95	−1.95
Mandibular								
Primary teeth								
Central incisor	0.31	0.00	−0.31	0.00	−1.00	−0.67		
Lateral incisor	1.21	1.52	0.00	−0.30	−0.83	−1.39		
Cuspid	0.31	0.31	−0.31	−0.63	−0.33	0.00	1.00	1.33
First molar	−1.30	−1.52	−1.30	−1.30	−0.60	−0.40	0.20	0.00
Second molar	1.04	1.04	−1.88	−1.46	0.00	−0.20	0.98	1.18
Permanent teeth								
Central incisor							−0.56	−0.83
Lateral incisor							−0.51	0.00
First molar							1.50	1.83

Tooth size represents the distance from the medial to the distal. Unit, S.D.

(RASopathies), including Noonan syndrome, CFC syndrome and Costello syndrome. However, a detailed investigation about craniofacial and dental findings has not yet been done. Recently, Goodwin et al. (2012) studied craniofacial and dental development in CFC syndrome based on 32 patients as the first large cohort study and found characteristic findings of the syndrome, including macrocephaly, convex facial profile, malocclusion with open bite, posterior cross bite, dental crowding, and high-arched palate. Among these features of CFC syndrome, macrocephaly, convex facial profile, malocclusion and high-arched palate were features noted in our patients with Costello syndrome as well. Unfortunately, as the evaluations of CFC syndrome by Goodwin et al. were mainly based on physical examination, more detailed evaluation regarding, such as dental arches, tooth size, and relationships between craniofacial, dental and skeletal structures have not been fully provided.

We used MDCT as a substitute for cephalometric, panoramic and dental cast studies. To our knowledge, this is the first study of thorough craniofacial and dental evaluation by using MDCT in Costello syndrome. As intellectual disability is common in Costello syndrome, these conventional cephalometric, panoramic and dental

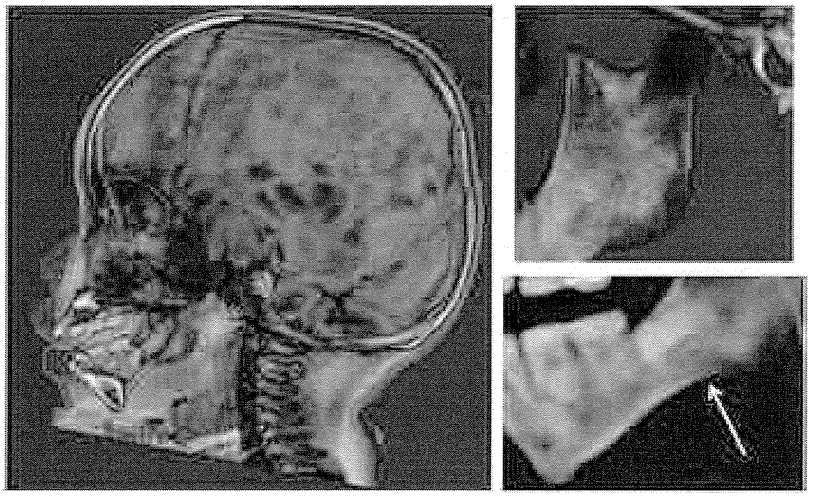

Fig. 4 Multi-detector row computed tomography (MDCT)-synthesized lateral radiograph (left) and close view of mandible (right) of Patient 3 at age of 6 years. Note the macrocephalic skull with hypoplastic facial bones (left). Mandibular anomalies are also noted, characterized by thick and flat head of the condylar process, short condylar neck, narrow mandibular notch (right upper) and antegonial notching (right lower).

Table 5 Lateral cephalometric analysis with MDCT of four patients

Patient	1	2	3	4
Skeletal				
Convexity	7.85	3.47	5.29	0.50
A-B plane	−0.12	−0.95	−1.78	0.76
SNA	4.06	−1.78	−1.78	−1.21
SNB	0.42	−2.89	−2.61	−1.14
Facial angle	−1.39	−1.54	1.39	0.53
SNP	−1.14	−2.99	−3.13	−1.56
Y axis	0.00	−0.15	−0.45	−0.84
SN-S·Gn	0.06	1.68	3.29	1.40
Mandibular plane	1.18	0.00	0.74	0.94
Gonial angle	0.77	−1.23	0.29	0.93
GZN	−0.12	2.33	2.51	2.09
FH to SN	−0.38	1.97	3.98	2.16
Dental				
U-1 to FH plane	2.37	−2.62	−0.31	4.44
U-1 to SN plane	3.12	−1.10	−2.41	3.02
L-1 to mandibular	1.17	4.94	−1.88	−1.28
Interincisal	−3.04	−2.04	0.80	−2.41
Occlusal plane	2.36	1.17	−0.69	−1.23

Unit, S.D.

cast studies are often difficult to perform, especially in the infantile period when patients tend to show marked irritability. MDCT is a useful tool for precise evaluation of craniofacial and oral manifestations in multiple congenital anomaly/intellectual disability syndromes (Hirai et al. 2011).

In conclusion, characteristic craniofacial and oral features frequently noted in patients with Costello syndrome might be true/relative macrocephaly with facial bone hypoplasia, gingival hypertrophy, malocclusion, occlusal attrition, small dental arches, microdontia, and convex face. Craniofacial and dental abnormalities are common in Costello syndrome patients and comprehensive dental care should be provided from early infancy.

ACKNOWLEDGMENTS

The authors are grateful to Professor Takahide Maeda for his helpful advice. We also thank Dr Kensuke Matsune, Dr Kenji Shimizu, Dr Yasuo Takahashi, and Hitoshi Yabe for their invaluable assistance. This study was funded in part by a Grant for the Support of Projects for Strategic Research at Private Universities by the Ministry of Education, Culture, Sports, Science and Technology (MEXT; 2008–2012), and by a grant from the Ministry of Health, Labour and Welfare, Japan.

REFERENCES

Abe Y, Aoki Y, Kuriyama S et al. 2012. Prevalence and clinical features of Costello syndrome and cardio-facio-cutaneous syndrome in Japan: findings from a nationwide epidemiological survey. Am J Med Genet A 158A:1083–1094.

Aoki Y, Niihori T, Kawame H et al. 2005. Germline mutations in HRAS proto-oncogene cause Costello syndrome. Nat Genet 37:1038–1040.

Becker MH, Coccaro PJ, Converse JM. 1976. Antegonial notching of the mandible: an often overlooked mandibular deformity in congenital and acquired disorders. Radiology 121:149–151.

Delrue MA, Chateil JF, Arveiler B, Lacombe D. 2003. Costello syndrome and neurological abnormalities. Am J Med Genet A 123A:301–305.

Der Kaloustian VM, Moroz B, McIntosh N, Watters AK, Blaichman S. 1991. Costello syndrome. Am J Med Genet 41:69–73.

Di Rocco M, Gatti R, Gandullia P, Barabino A, Picco P, Borrone C. 1993. Report on two patients with Costello syndrome and sialuria. Am J Med Genet 47:1135–1140.

van Eeghen AM, van Gelderen I, Hennekam RC. 1999. Costello syndrome: report and review. Am J Med Genet 82:187–193.

Fukawa A. 2008. Orthodontic consideration of quadruplets, compared to themselves and their parent at dento-maxilla-faical form. J Jpn Assoc Orthod 19:21–29.

Goodwin AF, Oberoi S, Landan M et al. 2012. Craniofacial and dental development in cardio-facio-cutaneous syndrome: the importance of ras signaling homeostasis. Clin Genet Sep 4. doi: 10.1111/cge.12005. [Epub ahead of print].

Hennekam RC. 2003. Costello syndrome: an overview. Am J Med Genet C Semin Med Genet 117C:42–48.

Hirai N, Yamauchi T, Matsune K et al. 2010. A comparison between two dimensional and three dimensional cephalometry on lateral radiographs and multi detector row computed tomography scans of human skulls. Int J Oral Med Sci 9:101–107.

Hirai N, Matsune K, Ohashi H. 2011. Craniofacial and oral features of Sotos syndrome: differences in patients with submicroscopic deletion and mutation of NSD1 gene. Am J Med Genet A 155A:2933–2939.

Iizuka T, Ishikawa F. 1957. Normal standards for various cephalometric analysis in Japanese adults. Nippon Kyosei Shika Gakkai Zasshi 16:4–12.

Johnson JP, Golabi M, Norton ME et al. 1998. Costello syndrome: phenotype, natural history, differential diagnosis, and possible cause. J Pediatr 133:441–448.

Kato K. 1979. [Studies on growth and development of dentition in Japanese children – examination of the longitudinal casts from deciduous dentition of 3-year-old to permanent dentition (author's transl)]. Shika Gakuho 79:991–1027. (In Japanese.)

Kawame H, Matsui M, Kurosawa K et al. 2003. Further delineation of the behavioral and neurologic features in Costello syndrome. Am J Med Genet A 118A:8–14.

Otsubo J. 1964. A longitudinal study of dental development between 6–13 years of age: growth changes of dentition. Nippon Kyosei Shika Gakkai Zasshi 23:182–190.

Rauen KA, Schoyer L, McCormick F et al. 2010. Proceedings from the 2009 genetic syndromes of the Ras/MAPK pathway: from bedside to bench and back. Am J Med Genet A 152A:4–24.

Teebi AS, Shaabani IS. 1993. Further delineation of Costello syndrome. Am J Med Genet 47:166–168.

Yamauchi T, Hirai N, Matsune K et al. 2010. Accuracy of tooth development stage, tooth size and dental arch width in multi detector row computed tomography scans of human skulls. Int J Oral Med Sci 9:108–114.

Zampino G, Mastroiacovo P, Ricci R et al. 1993. Costello syndrome: further clinical delineation, natural history, genetic definition, and nosology. Am J Med Genet 47:176–183.

RESEARCH ARTICLE

AMERICAN JOURNAL OF medical genetics PART A

Craniofacial and Oral Features of Sotos Syndrome: Differences in Patients With Submicroscopic Deletion and Mutation of *NSD1* Gene

Norimitsu Hirai,[1]* Kensuke Matsune,[2] and Hirofumi Ohashi[3]

[1]Department of Pediatric Dentistry, Nihon University Graduate School of Dentistry at Matsudo, Chiba, Japan

[2]Department of Pediatric Dentistry, Nihon University School of Dentistry at Matsudo, Chiba, Japan

[3]Division of Medical Genetics, Saitama Children's Medical Center, Saitama, Japan

Received 7 October 2010; Accepted 22 January 2011

Sotos syndrome is a well known overgrowth syndrome caused by haploinsufficiency of *NSD1* gene located at 5q35. There are two types of mutations that cause *NSD1* haploinsufficiency: mutations within the *NSD1* gene (mutation type) and a 5q35 submicroscopic deletion encompassing the entire *NSD1* gene (deletion type). We investigated detailed craniofacial, dental, and oral findings in five patients with deletion type, and three patients with mutation type Sotos syndrome. All eight patients had a high palate, excessive tooth wear, crowding, and all but one patient had hypodontia and deep bite. Hypodontia was exclusively observed in the second premolars, and there were no differences between the deletion and mutation types in the number of missing teeth. Another feature frequently seen in common with both types was maxillary recession. Findings were more frequent and more pronounced in deletion type than in mutation type included mandibular recession, scissors or posterior cross bite, and small dental arch with labioclination of the maxillary central incisors. It is noteworthy that although either scissors bite or crossbite was present in all of the deletion-type patients, neither of these was observed in mutation-type patients. Other features seen in a few patients include enamel hypoplasia (two deletion patients), and ectopic tooth eruption (one deletion and one mutation patients). Our study suggests that Sotos syndrome patients should be observed closely for possible dental and oral complications especially for malocclusion in the deletion type patients. © 2011 Wiley Periodicals, Inc.

Key words: Sotos syndrome; *NSD1*; submicroscopic deletion; small dental arch; malocclusion; mandibular recession

How to Cite this Article:
Hirai N, Matsune K, Ohashi H. 2011. Craniofacial and oral features of Sotos syndrome: differences in patients with submicroscopic deletion and mutation of *NSD1* gene.
Am J Med Genet Part A 155:2933–2939.

INTRODUCTION

Sotos syndrome is a congenital genetic disorder characterized by overgrowth starting before birth, specific facial manifestations (macrocephaly, prominent forehead, hypertelorism, downslanting palpebral fissures, and pointed chin), advanced bone age, and developmental impairment. Since its initial description by Sotos et al. [1964] several hundred patients have been reported to date. It may be accompanied by a variety of complications, including cardiovascular, urinogenital, and ophthalmic malformations, skeletal abnormalities, and seizures. Dental and oral findings have been reported to include premature tooth eruption, hypodontia, enamel hypoplasia, excessive tooth wear, maxillary and mandibular recession, talon cusps, fused teeth, and expanded pulp cavity of deciduous teeth [Welbury and Fletcher, 1988; Cole and Hughes, 1994; Inokuchi et al., 2001; Gomes-Silva et al., 2006; Takei et al., 2007; Nishimura et al., 2008].

Kurotaki et al. [2002] reported that this syndrome is caused by haploinsufficiency of the *NSD1* nuclear receptor SET domain containing protein 1 gene located on 5q35. There are two main types that cause *NSD1* haploinsufficiency: mutations within the *NSD1* gene, and a submicroscopic deletion in the region that contains the *NSD1* gene (constant deletion of approximately 2.2Mb including *NSD1* and around 20 neighboring genes) [Kurotaki et al., 2002]. Nagai et al. [2003] investigated differences in clinical manifestations between these two types, and reported

Grant sponsor: Ministry of Education, Culture, Sports, Science and Technology (MEXT); Grant number: 2008-2012; Grant sponsor: Ministry of Health, Labour and Welfare, Japan.

*Correspondence to
Norimitsu Hirai, Department of Pediatric Dentistry, Nihon University Graduate School of Dentistry at Matsudo, 2-870-1 Sakaecho-Nishi, Matsudo, Chiba 271-8587, Japan. E-mail: hirai.norimitsu@nihon-u.ac.jp

Published online 19 October 2011 in Wiley Online Library (wileyonlinelibrary.com)
DOI 10.1002/ajmg.a.33969

that major anomalies such as central nervous, cardiovascular, and urinogenital abnormalities are more common in the deletion-type. Their only reference to dental findings, however, stated that early tooth eruption occurred in both types with no significant difference.

The first detailed investigation of dental and oral findings seen in Sotos syndrome based on *NSD1* genetic diagnosis was carried out by Kotilainen et al. [2009]. They analyzed dental and oral findings from 13 patients with Sotos syndrome (all except one with the mutation type), including panoramic imaging, and reported the characteristic oral complications of Sotos syndrome, including hypodontia of the second premolars. We here report on the results of our investigation of detailed craniofacial, dental, and oral findings in five patients with deletion-type, and three patients with mutation-type Sotos syndrome.

MATERIALS AND METHODS

Patients

The eight patients comprised a group who underwent examination at Saitama Children's Medical Center. Five patients (three males, two females; age, 6–13 years) were identified as having a submicroscopic deletion on 5q35 including the *NSD1* gene, and three (all females; age, 6–10 years) were identified as having a mutation of the *NSD1* gene. Deletions were identified by fluorescence in situ hybridization (FISH) analysis of metaphase chromosomes from peripheral blood, using a total of seven bacterial artificial chromosome (BAC) clones comprising the BAC clone that includes the *NSD1* gene (RP11-99N22) together with those toward the centromere (RP11-880A16, RP11-69018, RP11-991B23) and toward the telomere (RP11-147K7, RP11-452O4, and RP11-158F10). The results showed that the same ~2 Mb deletion was present in all five patients. Mutation analysis using genomic DNA extracted from peripheral blood was performed by polymerase chain reaction (PCR) and direct sequencing of all translated regions for exon 2–23. The results identified mutations generating premature termination in both Patients 6 and 7, comprising a five base deletion (2053–2057delAAGTA) and a base deletion (5431delC), respectively, and a missense mutation (4991G>C) in Patient 8. Details of clinical manifestations are shown in Table I. This study protocol was approved by the Ethics Committee of Saitama Children's Medical Center and proper informed consents were obtained from the legal guardians of the patients.

Oral and Dental Studies

Physical examination and dental cast studies were used to evaluate palatal morphology, tooth calcification, dental arches, occlusion, tooth size, and tooth eruption status. Panoramic and lateral cephalometric radiographs reconstructed from multi-detector row computed tomography (MDCT) were also used to evaluate the relationship of craniofacial, dental and skeletal structures, and hypodontia [Hirai et al., 2010; Yamauchi et al., 2010]. Crown and

TABLE I. Clinical Manifestations of Eight Patients With Sotos Syndrome

	Deletion type patients					Mutation type patients		
	1	2	3	4	5	6	7	8
Gender	M	F	F	M	M	F	F	F
Ages (years)	7	8	6	7	13	7	10	6
Overgrowth	–	–	–	–	–	+	+	+
Intellectual disability	Moderate	Moderate	Moderate	Moderate	Moderate	Mild	–	Mild
Seizure	–	+	–	+	–	–	+	–
Craniofacial features								
Macrocephaly	+	+	+	–	+	+	+	–
Prominent forehead	+	+	+	+	+	+	+	–
Hypertelorism	+	+	+	+	+	+	+	+
Downslanting palpebral fissures	+	+	+	+	+	+	–	+
Pointed chin	+	+	+	+	+	+	–	+
Strabismus	+	+	+	–	–	+	–	–
Skeletal anomaly								
Scoliosis	–	–	–	+	+	–	+	+
Pes planovalgus	+	–	+	+	+	+	–	+
Cardiovascular anomaly	AR	PDA	–	PDA, ASD, VSD	–	VSD, CoA	MR	–
Urogenital anomaly	Hydronephrosis, VUR	–	–	–	–	Urethrocele	Hydronephrosis, hydroureter	–
Others	Hearing loss	Myelomeningocele, umbilical hernia	–	–	–	–	–	–

M, male; F, female; AR, aortic regurgitation; PDA, patent ductus arteriosus; ASD, atrial septal defect; VSD, ventricular septal defect; CoA, coarctation of aorta; MR, mitral regurgitation; VUR, vesicoureteral reflux; +, present; –, absent.

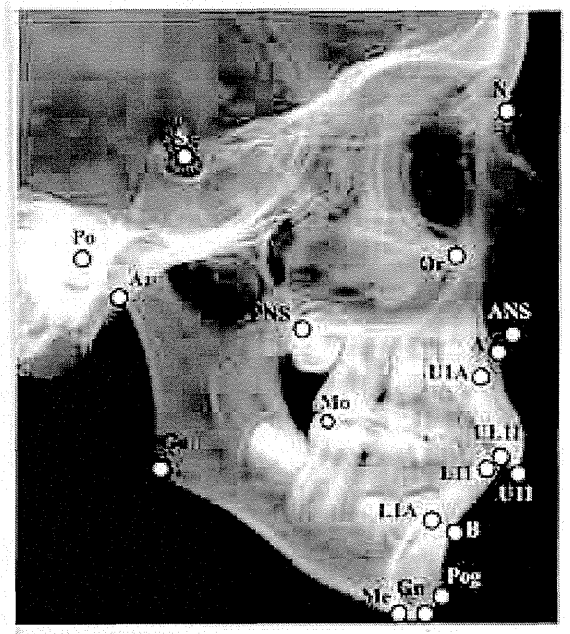

FIG. 1. Landmark points, angles, and lines used in cephalometoric analysis and profilogram. Landmarks: N, nasion; Or, orbitale; S, sella turcia; Po, porion; Ar, articulare; Go, gonion; Me, mentor; Gn, gnathion; Pog, pogonion; A, A-point; B, B-point; ANS, anterior nasal spine; Mo, molar occlusion; U1A, upper central incisor root apex; U1I, upper central incisor edge; L1A, lower central incisor root apex; L1I, lower central incisor edge; UL1I, middle of U1I and L1I. Angles: convexity, N-A line to the A-Pog line; A-B plane, N-Pog line to the A-B line; SNA, S-N line to the N-A line; SNB, S-N line to the N-B line; facial angle, Po-Or line to the N-Pog line; SNP, S-N line to the N-Pog line; y-axis, Po-Or line to the S-Gn line; SN-S Gn, S-N line to the S-Gn line; mandibular plane, Po-Or line to the Me-the lower border of the mandible line; gonial angle, Ar-the posterior border of the ramus of the mandible line to the Me-the lower border of the mandible line; GZN, S-N line to the Ar-the posterior border of the ramus of the mandible line; FH to SN, Po-or line to the S-N line; U-1 to FH plane, U1I-U1A line to the Po-or line; IP-1 to SN plane, U1I-U1A line to the S-N line; L-1 to mandibular, L1I-L1A line to the Me-the lower border of the mandible; interincisal, U1I-U1A line to the L1I-L1A line; occlusal plane, Po-Or line to the Mo-UL1I line.

dental arch sizes were measured using a caliper with a resolution accuracy of 0.01 mm. Lateral cephalometric analysis was performed based on the method developed by Iizuka and Ishikawa [1957] (Fig. 1). All data in this study (tooth size, dental arch form size, and cephalometric findings) were compared with standard values for Japanese individuals [Otsubo, 1957; Otsubo et al., 1964].

RESULTS

Oral and dental anomalies noted in eight patients are summarized in Table II. All eight patients had a high palate, crowding, and excessive tooth wear. All but one (Patient 1 with *NSD1* deletion) had hypodontia exclusively in the second premolars. There were no differences between the deletion-type and mutation-types in the number of missing teeth (mean number of missing teeth was 2 in the deletion-type and 2.6 in the mutation-type) (Fig. 2). The results of cephalometric analysis showed that among the five deletion-type patients, maxillary and mandibular recession was present in three and maxillary recession alone in one, whereas among the three mutation-type patients maxillary and mandibular recession was present in one and maxillary recession alone in one. The deletion-type was regarded as having a stronger tendency for mandibular recession (Table III). In terms of occlusion, crowding was present in all patients, and deep bite was seen in all but one (Patient 2 with *NSD1* deletion). It is noteworthy that although either scissors bite (Patients 1, 3, and 4) or cross bite (Patients 2 and 5) was present in all of the deletion-type patients, neither of these was observed in mutation-type patients (Fig. 3).

Small dental arch was present in all the deletion-type patients and one mutation-type patient (Table IV). In terms of morphological categories of small dental arch, the maxilla exhibited a narrow dental arch with labioclination of the central incisors in all five deletion-type patients, with the mandible being saddle-shaped in three patients and U-shaped in two, while the mutation-type patient had U-shaped upper and lower dental arches (Fig. 4). In terms of tooth size, both microdontia and macrodontia were occasionally seen in both the deletion-type and mutation-types, but no characteristic findings were present in either type (data not shown). Enamel hypoplasia was present in two out of the five deletion-type patients (Patients 2 and 3), but was not present in the mutation-type. In addition, ectopic eruptions of the first molar was present in one deletion-type patient (Patient 4, right mandibular) and one mutation-type patient (Patient 6, bilateral maxillary). Some representative photographs of oral and dental anomalies noted in patients studied are shown in Figure 5.

DISCUSSION

The oral manifestations observed in common with both deletion and mutation type Sotos syndrome patients noted here were a high palate, excessive tooth wear, recession of maxilla, deep bite, crowding, and hypodontia. Hypodontia has been previously described by several authors [Inokuchi et al., 2001; Callman et al., 2006; Gomes-Silva et al., 2006; Nishimura et al., 2008]. Kotilainen et al. [2009] recently investigated 13 patients with Sotos syndrome (12 patients with *NSD1* mutations and one with *NSD1* deletion) and found one or more premolar teeth were absent in 9 out of 13 patients (8 out of 12 mutation patients and one deletion-type patient). Based on the observation that the deletion patient had the most severe phenotype of tooth agenesis, involving not only the second premolars and the third molars, but also one mandibular incisor, they noted the possibility that patient with the *NSD1* deletion had the most severe tooth agenesis. In our study, however, which included five deletion-type patients, although similar high rates of hypodontia were observed in both the deletion-type and mutation-type, we did not observe any difference in severity in either the deletion-type or mutation-type.

One noteworthy difference between the deletion-type and mutation-type was the fact that either scissors bite or cross bite

TABLE II. Oral and Dental Anomalies in Eight Patients

	Deletion type patients					Mutation type patients			Total	
Oral anomalies	1	2	3	4	5	6	7	8	Deletion type	Mutation type
High palate	+	+	+	+	+	+	+	+	5/5	3/3
Excessive tooth wear	+	+	+	+	+	+	+	+	5/5	3/3
Hypodontia	−	+	+	+	+	+	+	+	4/5	3/3
Maxillary recession	+	−	+	+	+	+	+	−	4/5	2/3
Mandibular recession	−	−	+	+	+	−	+	−	3/5	1/3
Malocclusion										
Scissors bite	+	−	+	+	−	−	−	−	3/5	0/3
Cross bite	−	+	−	−	+	−	−	−	2/5	0/3
Deep bite	+	−	+	+	+	+	+	+	4/5	3/3
Crowding	+	+	+	+	+	+	+	+	5/5	3/3
Small dental arch	+	+	+	+	+	−	+	−	5/5	1/3
Maxilla	N	N	N	N	N	U	U	U		
Mandibula	S	U	S	S	U	U	U	U		
Labioclination of maxillary central incisor	+	+	+	+	+	−	−	−	5/5	0/3
Enamel hypoplasia	−	+	+	−	−	−	−	−	2/5	0/3
Ectopic tooth eruption	−	−	−	+	−	+	−	−	1/5	1/3

N, narrow dental arch; U, U-shaped dental arch; S, saddle-shaped dental arch; +, present; −, absent.

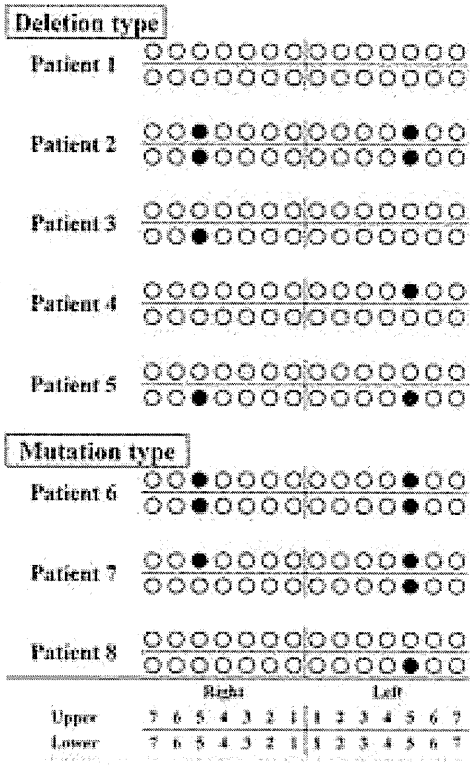

FIG. 2. Hypodontia in eight patients with Sotos syndrome. ●, Congenitally missing teeth.

was observed in all deletion-type patients, whereas neither was present in the mutation-type. All of the deletion-type patients had small dental arches, and in terms of morphological categories, the maxilla exhibited a narrow dental arch with labioclination of the central incisors in all five deletion-type patients, with the mandible being saddle-shaped in three patients and U-shaped in two. Only one single mutation-type patient had small dental arches with both upper and lower dental arches being U-shaped. Narrowing of the dental arch is more pronounced in the narrow-shape and saddle-shape compared with the U-shape. It is possible that the degree of narrowing of the dental arch in the deletion-type and the misalignment in arch morphology between the maxilla and mandible causes scissors bite or cross bite.

In addition, maxillary and mandibular recession has also been reported as a dental manifestation of Sotos syndrome [Welbury and Fletcher, 1988; Takei et al., 2007]. In our results, there was a tendency toward maxillary and mandibular recession in the deletion-type and maxillary recession in the mutation-type. Based on these findings, there was a tendency for maxillary recession to occur in both the deletion-type and mutation-type, but there was also a tendency toward the occurrence of mandibular recession in the deletion-type. Taken in conjunction with the pronounced mandibular recession seen in the deletion-type on cephalometric analysis, mandibular malformations, including those of the dental arch, may be regarded as characteristic of the deletion-type. The cause is unknown, but in the deletion-type, minute genomic imbalances, involving considerable number of genes other than the *NSD1* gene, may either: (1) directly cause deficient growth of the mandibular area; or (2) secondarily cause malocclusion or abnormal dental arch morphology as a result of dysfunction of the perioral muscles associated with more

TABLE III. Lateral Cephalometric Analyses With MDCT of Eight Patients

	Deletion type patients					Mutation type patients		
	1	2	3	4	5	6	7	8
Skeletal								
Convexity	−2.56	−1.05	−0.66	−1.80	−1.95	−4.56	−2.52	−2.94
A–B plane	−1.12	−3.96	1.68	−0.32	1.40	2.15	1.96	2.56
SNA	−2.54	1.24	−2.28	−3.45	−2.32	−2.69	−3.18	−1.63
SNB	−1.80	1.71	−3.31	−3.18	−2.84	−0.76	−2.29	−0.07
Facial angle	0.68	−3.23	−0.47	0.38	0.34	0.38	−1.55	1.43
SNP	−0.71	1.77	−1.76	−1.16	−0.63	0.02	−2.22	0.11
Y-axis	−0.50	−0.37	−0.38	−0.09	0.17	−0.36	1.29	−1.34
SN-S-Gn	3.08	−1.30	0.32	3.86	0.93	0.22	1.86	−0.30
Mandibular plane	1.29	1.05	−1.47	0.30	1.12	−0.58	1.98	−0.29
Gonial angle	6.24	−0.15	−4.06	−5.27	0.73	0.29	0.44	3.06
OZN	0.77	0.09	3.01	2.84	1.19	−0.37	1.52	−0.27
FH to SN	2.38	−1.15	0.71	2.55	0.98	0.52	0.97	1.37
Denture								
U-1 to FH plane	1.30	1.37	2.94	0.30	0.72	−0.47	0.50	0.69
U-1 to SN plane	0.51	1.87	2.56	−0.52	0.24	−0.64	−0.46	0.21
L-1 to mandibular	−2.24	−0.47	0.98	−1.47	−1.64	−2.39	−0.46	−1.93
Interincisal	−0.02	−1.07	−1.53	0.46	0.22	1.90	−0.83	0.71
Occlusal plane	−0.99	1.09	−0.76	−0.24	2.97	−1.37	1.35	−0.49

Unit: SD.

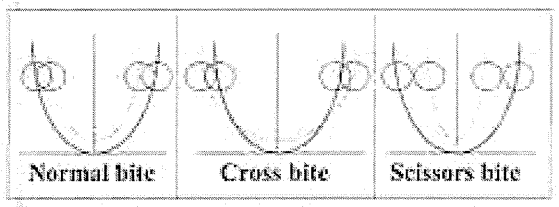

FIG. 3. Schematic representations of normal and abnormal occlusions. ——— , Maxillary dental arch; - - - - - - , mandibular dental arch; ◯ , maxillary first molar; ◯ , mandibular first molar.

pronounced developmental impairment [Grabowski et al., 2007a,b; Stahl et al., 2007].

Enamel hypoplasia has also been reported as a dental manifestation of Sotos syndrome [Inokuchi et al., 2001]. Kotilainen et al. [2009] reported enamel hypoplasia in four out of 13 patients (all mutation type). In our study, enamel hypoplasia was present in two out of five deletion-type patients, but not in any mutation-type patients. Enamel hypoplasia is thought to be a common manifestation that can occasionally occur in both the deletion-type and mutation-type rather than a manifestation that is prone to occur in either type.

As mild to moderate intellectual disability is common in Sotos syndrome, conventional panoramic and cephalometric studies

TABLE IV. Dental Arch Measurements in Eight Patients

	Deletion type patients					Mutation type patients		
	1	2	3	4	5	6	7	8
Maxillary								
W_c	−0.55	Deciduous	0.04	Deciduous	1.79	−1.75	0.61	−1.30
W_m	−3.76	−3.59	0.02	−4.18	−3.11	−1.73	−2.04	−1.76
L_{1d}	2.68	1.32	2.88	1.02	−0.69	1.44	0.14	−1.36
Mandibular								
W_c	Deciduous	Deciduous	−1.00	Deciduous	−0.73	−1.81	−2.70	−0.30
W_m	−4.82	−2.51	−2.16	−4.45	−3.38	−1.57	−4.34	0.96
L_{1d}	0.81	1.32	1.85	0.63	−3.40	0.28	−2.07	0.56

Unit: SD.

The W_c and W_m represent the distance between the primary canines (the cuspids), and the first molars, respectively. The L_{1d} represents the length from the mesial surface of the first molars to central point of incisors.

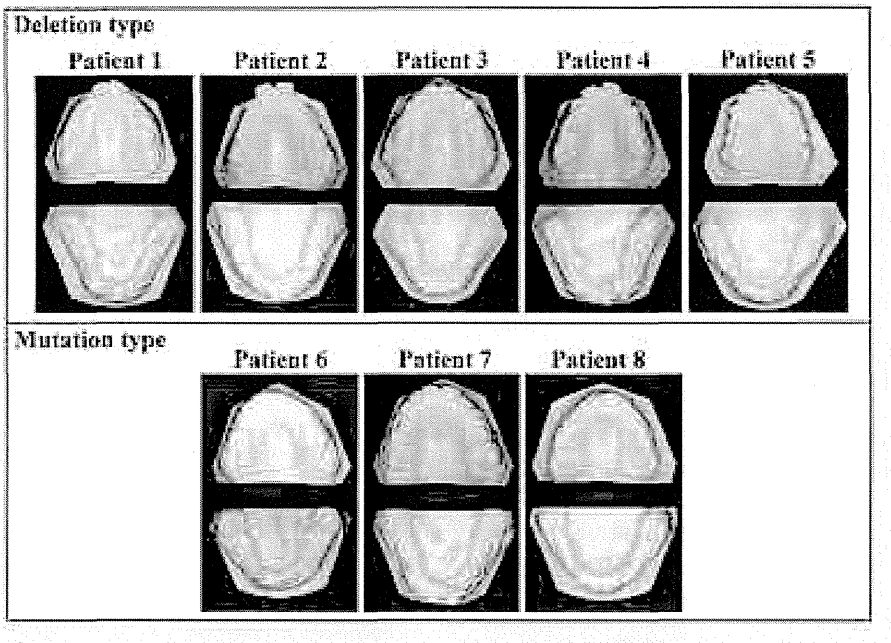

FIG. 4. Dental arch shapes of eight patients. Upper panel: maxillary dental casts, lower panel: mandibular dental casts. A narrow maxillary dental arch with labioclination of the central incisors is noted in all five deletion type patients, with the mandibula being saddle-shaped in three patients (Patients 1, 3, and 4) and U-shaped in two (Patients 2 and 5), while U-shaped upper and lower dental arches are noted in all three mutation-type patients (Patients 6, 7, and 8).

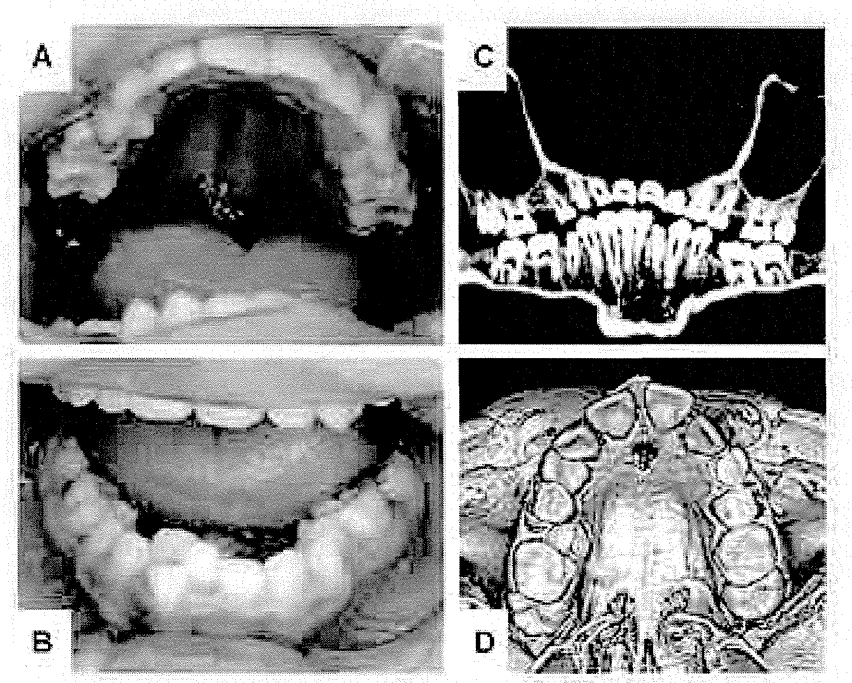

FIG. 5. Oral photographs (A,B) and MDCT-synthesized panoramic radiograph (C) of Patient 7 at age of 10 years and MDCT-synthesized upper dental arch of Patient 6 at age of 7 years (D). Note: high palate, malocclusion, small dental arch, excessive tooth wear (A,B), missing upper second premolars on both side and lower left second premolar (C), ectopic tooth eruption of first molars on both side (D).

were often difficult to perform in childhood. Thus, in this study, MDCT was used as a substitute for cephalometric radiographs and panoramic radiographs, and by which maxillofacial manifestations could be accurately evaluated [Hirai et al., 2010; Yamauchi et al., 2010].

In view of oral and dental management, we would like to provide recommendations as follows: periodic dental check up to prevent dental caries or gingivitis should be started early after one or more deciduous teeth have erupted. Around age 7 years, detailed oral and dental evaluations, including dental cast studies and MDCT, is recommended for possible hypodontia and malocclusion. If the patient has hypodontia, preceding deciduous tooth (teeth) should be maintained as long as possible with proper care. Although malocclusion like scissors bite and cross bite requires early treatment, including expansion of upper or lower jaw, to prevent craniofacial disabilities such as facial asymmetry and temporomandibular joint dysfunction, the treatment should be carefully decided based on consideration of capability of cooperation of the patients.

In conclusion, features seen more frequently and more pronounced form in deletion-type than in mutation-type were small dental arch with labioclination of the maxillary central incisors, mandibular recession, and scissors or posterior cross bite. Sotos syndrome patients should be followed closely for possible dental and oral complications especially for malocclusion in the deletion-type.

ACKNOWLEDGMENTS

The authors are grateful to Prof. Takahide Maeda for his helpful advice. We also thank to Dr. Kenji Shimizu, Dr. Yasuo Takahashi, and Hitoshi Yabe for their invaluable assistance. This study was funded in part by a Grant for the Support of Projects for Strategic Research at Private Universities by the Ministry of Education, Culture, Sports, Science and Technology (MEXT; 2008-2012), and by a grant from the Ministry of Health, Labour and Welfare, Japan.

REFERENCES

Cullinan AP, Anand P, Sheehy EC. 2006. Sotos syndrome with hypodontia. Inter J Paediatri Dent 16:143–146.

Cole TRP, Hughes HE. 1994. Sotos syndrome: A study of the diagnostic criteria and natural history. J Med Genet 31:20–32.

Gomes-Silva JM, Ravicese DB, Segatto RA, de Queiroz AM, de Freitas AC. 2006. Sotos syndrome: A case report. Spec Care Dentist 26:257–262.

Grabowski R, Kundt G, Stahl F. 2007a. Interrelation between occlusal findings and orofacial myofunctional status in primary and mixed dentition: Part III: Interrelation between malocclusions and orofacial dysfunctions. J Orofac Orthop 68:462–476.

Grabowski R, Stahl F, Gaebel M, Kundt G. 2007b. Relationship between occlusal findings and orofacial myofunctional status in primary and mixed dentition. Part I: Prevalence of malocclusions. J Orofac Orthop 68:26–37.

Hirai N, Yamauchi T, Matsune K, Kobayashi R, Yabe H, Ohashi H, Maeda T. 2010. A comparison between two dimensional and three dimensional cephalometry on lateral radiographs and multi detector row computed tomography scans of human skulls. Int J Oral-Med Sci 9:101–107.

Iizuka T, Ishikawa F. 1957. Normal standards for various cephalometric analysis in Japanese adults. Nippon Kyosei Shika Gakkai Zasshi 16:4–12.

Imaeuchi M, Nomura J, Matsumura Y, Sekida M, Tagawa T. 2001. Sotos syndrome with enamel hypoplasia: A case report. J Clin Pediatr Dent 25:313–316.

Kotulainen L, Pohjola P, Pirinen S, Arte S, Nieminen P. 2009. Premolar hypodontia is a common feature in Sotos syndrome with a mutation in the NSD1 gene. Am J Med Genet Part A 149A:2409–2414.

Kurotaki N, Imaizumi K, Harada N, Masuno M, Kondoh T, Nagai T, Ohashi H, Naritomi K, Tsukahara M, Makita Y, Sugimoto T, Sonoda T, Hasegawa T, Chinen Y, Tomita HH, Kinoshita A, Yoshiura KK, Ohta T, Kishino T, Fukushima Y, Niikawa N, Matsumoto N. 2002. Haploinsufficiency of NSD1 causes Sotos syndrome. Nat Genet 30:365–366

Nagai T, Matsumoto N, Kurotaki N, Harada N, Niikawa N, Ogata T, Imaizumi K, Kurosawa K, Kondoh T, Ohashi H, Tsukahara M, Makita Y, Sugimoto T, Sonoda T, Yokoyama T, Uetake K, Sakazume S, Fukushima Y, Naritomi K. 2003. Sotos syndrome and haploinsufficiency of NSD1: Clinical features of intragenic mutations and submicroscopic deletions. J Med Genet 40:285–289.

Nishimura K, Mori Y, Yamauchi M, Kamakura N, Homma H, Namura H, Miyamoto E, Matsumoto M, Shintani S, Ooshima T. 2008. Sotos syndrome with oligodontia: A case report. Pediatric Dent J 18:187–191.

Otsuka I. 1957. A study on the tooth material in Japanese adults of normal occlusion. its relationship to coronal and basal arches. Nippon Kyosei Shika Gakkai Zasshi 16:36–46.

Otsuka I, Ishikawa F, Kuwahara Y. 1964. A longitudinal study of dental development between 6–13 years of age: Growth changes of dentition. Nippon Kyosei Shika Gakkai Zasshi 23:182–190.

Sotos JF, Dodge PR, Muirhead D, Crawford JD, Talbot NB. 1964. Cerebral gigantism in childhood. A syndrome of excessively rapid growth with acromegalic features and a nonprogressive neurologic disorder. N Engl J Med 271:109–116

Stahl F, Grabowski R, Gaebel M, Kundt G. 2007. Relationship between occlusal findings and orofacial myofunctional status in primary and mixed dentition. Part II: Prevalence of orofacial dysfunctions. J Orofac Orthop 68:574–90

Takei K, Suzuki K, Yamaguchi H, Ohtawa Y. 2007. Dentofacial growth in patients with Sotos syndrome. Bull Tokyo Dent Coll 48:73–85.

Welbury RR, Fletcher HI. 1988. Cerebral gigantism (Sotos syndrome) two case reports. J Paediatr Dent 4:41–44

Yamauchi T, Hirai N, Matsune K, Kobayashi R, Yabe H, Ohashi H, Maeda T. 2010. Accuracy of tooth development stage, tooth size and dental arch width in multi detector row computed tomography scans of human skulls. Int J Oral Med Sci 9:106–114.

Mutations in *B3GALT6*, which Encodes a Glycosaminoglycan Linker Region Enzyme, Cause a Spectrum of Skeletal and Connective Tissue Disorders

Masahiro Nakajima,[1,21] Shuji Mizumoto,[2,21] Noriko Miyake,[3,21] Ryo Kogawa,[2] Aritoshi Iida,[1] Hironori Ito,[4] Hiroshi Kitoh,[5] Aya Hirayama,[6] Hiroshi Mitsubuchi,[7] Osamu Miyazaki,[8] Rika Kosaki,[9] Reiko Horikawa,[10] Angeline Lai,[11] Roberto Mendoza-Londono,[12] Lucie Dupuis,[12] David Chitayat,[12] Andrew Howard,[13] Gabriela F. Leal,[14] Denise Cavalcanti,[15] Yoshinori Tsurusaki,[3] Hirotomo Saitsu,[3] Shigehiko Watanabe,[16] Ekkehart Lausch,[17] Sheila Unger,[18] Luisa Bonafé,[19] Hirofumi Ohashi,[16] Andrea Superti-Furga,[19] Naomichi Matsumoto,[3] Kazuyuki Sugahara,[2] Gen Nishimura,[20] and Shiro Ikegawa[1,*]

Proteoglycans (PGs) are a major component of the extracellular matrix in many tissues and function as structural and regulatory molecules. PGs are composed of core proteins and glycosaminoglycan (GAG) side chains. The biosynthesis of GAGs starts with the linker region that consists of four sugar residues and is followed by repeating disaccharide units. By exome sequencing, we found that *B3GALT6* encoding an enzyme involved in the biosynthesis of the GAG linker region is responsible for a severe skeletal dysplasia, spondyloepimetaphyseal dysplasia with joint laxity type 1 (SEMD-JL1). *B3GALT6* loss-of-function mutations were found in individuals with SEMD-JL1 from seven families. In a subsequent candidate gene study based on the phenotypic similarity, we found that *B3GALT6* is also responsible for a connective tissue disease, Ehlers-Danlos syndrome (progeroid form). Recessive loss-of-function mutations in *B3GALT6* result in a spectrum of disorders affecting a broad range of skeletal and connective tissues characterized by lax skin, muscle hypotonia, joint dislocation, and spinal deformity. The pleiotropic phenotypes of the disorders indicate that *B3GALT6* plays a critical role in a wide range of biological processes in various tissues, including skin, bone, cartilage, tendon, and ligament.

Skeletal dysplasias represent a vast collection of genetic disorders of the skeleton, currently divided into 40 groups.[1] Spondyloepimetaphyseal dysplasia (SEMD) is one group (group 13) of skeletal dysplasia that contains more than a dozen distinctive diseases. SEMD with joint laxity (SEMD-JL) is a subgroup of SEMD that consists of type 1 (SEMD-JL1 [MIM 271640]) and type 2 (SEMD-JL2 [MIM 603546]). SEMD-JL1 or SEMD-JL Beighton type is an autosomal-recessive disorder that shows mild craniofacial dysmorphism (prominent eye, blue sclera, long upper lip, small mandible with cleft palate) and spatulate finger with short nail.[2] The large joints of individuals with SEMD-JL1 are variably affected with hip dislocation, elbow contracture secondary to radial head dislocation, and clubfeet. Joint laxity is particularly prominent in the hands. Skeletal changes of SEMD-JL1 are characterized by moderate platyspondyly with anterior projection of the vertebral bodies, hypoplastic ilia, and mild metaphyseal flaring.[3] Kyphoscoliosis progresses with age, leading to a short trunk, whereas platyspondyly become less conspicuous and the vertebral bodies appear squared in shape with age. Recently, dominant kinesin family member 22 (*KIF22* [MIM 603213]) mutations have been found in SEMD-JL2;[4,5] however, the genetic basis of SEMD-JL1 remains unknown.

To identify the SEMD-JL1-causing mutation, we performed whole-exome sequencing experiments. We recruited seven individuals with SEMD-JL1 from five unrelated Japanese families (F1–F5) and a Singapore/Japanese family (F6) (Table 1). One family (F1) had a pair of affected sibs (P1 and P2) from nonconsanguineous parents. Genomic DNA was extracted by standard procedures

[1]Laboratory for Bone and Joint Diseases, Center for Integrative Medical Sciences, RIKEN, Tokyo 108-8639, Japan; [2]Laboratory of Proteoglycan Signaling and Therapeutics, Frontier Research Center for Post-Genomic Science and Technology, Graduate School of Life Science, Hokkaido University, Sapporo 001-0021, Japan; [3]Department of Human Genetics, Yokohama City University Graduate School of Medicine, Yokohama 236-0004, Japan; [4]Department of Orthopaedic Surgery, Central Hospital, Aichi Prefectural Colony, Kasugai 480-0392, Japan; [5]Department of Orthopaedic Surgery, Nagoya University School of Medicine, Nagoya 466-8550, Japan; [6]Department of Pediatrics, Akita Prefectural Center on Development and Disability, Akita 010-1407, Japan; [7]Department of Neonatology, Kumamoto University Hospital, Kumamoto 860-8556, Japan; [8]Department of Radiology, National Center for Child Health and Development, Tokyo 157-8535, Japan; [9]Division of Medical Genetics, National Center for Child Health and Development, Tokyo 157-8535, Japan; [10]Division of Endocrinology and Metabolism, National Center for Child Health and Development, Tokyo 157-8535, Japan; [11]Department of Paediatric Medicine, KK Women's and Children's Hospital, Singapore 229899, Singapore; [12]Department of Paediatrics, The Hospital for Sick Children and University of Toronto, Toronto, ON M5G 1X8, Canada; [13]Department of Surgery, The Hospital for Sick Children and University of Toronto, Toronto, ON M5G 1X8, Canada; [14]The Professor Fernando Figueira Integral Medicine Institute (IMIP), Recife, PE 50070-550, Brazil; [15]Skeletal Dysplasia Group, Department of Medical Genetics, Faculty of Medical Sciences, State University of Campinas (UNICAMP), Campinas, SP 13083-970, Brazil; [16]Division of Medical Genetics, Saitama Children's Medical Center, Saitama 339-8551, Japan; [17]Division of Paediatric Genetics, Centre for Pediatrics and Adolescent Medicine, University of Freiburg, Freiburg 79106, Germany; [18]Medical Genetics Service, University of Lausanne, CHUV, Lausanne 1011, Switzerland; [19]Department of Pediatrics, University of Lausanne, CHUV, Lausanne 1011, Switzerland; [20]Department of Pediatric Imaging, Tokyo Metropolitan Children's Medical Center, Fuchu 183-8561, Japan
[21]These authors contributed equally to this work
*Correspondence: sikegawa@ims.u-tokyo.ac.jp
http://dx.doi.org/10.1016/j.ajhg.2013.04.003.

Table 1. Clinical and Radiographic Findings of the Individuals with *B3GALT6* Mutations

Subject ID	P1	P2	P3	P4	P5	P6	P7	P8	P9	P10	P11	P12
Family ID	F1	F1	F2	F3	F4	F5	F6	F7	F8	F9	F9	F10
Clinical diagnosis	SEMD-JL1	SEMD-JL1	SEMD-JL1	SEMD-JL1	SEMD-JL1	SEMD-JL1	SEMD-JL1	SEMD-JL1	EDS-PF	EDS-PF	EDS-PF	EDS-PF
General Information												
Ethnicity	Japanese	Japanese	Japanese	Japanese	Japanese	Japanese	Japanese/ Singaporean	Vietnamese	Italian	Italian/ Canadian	Italian/ Canadian	Brazilian
Gender	M	M	F	M	F	F	M	M	M	F	F	F
Age	34 years	31 years	12 years, 7 months	6 years	5 years, 1 month	12 years	2 years, 9 months	34 years	8 months	7 years	1 month	5 years, 1 month
Gestational age	39 weeks, 2 days	full term	37 weeks	40 weeks, 1 day	39 weeks, 5 days	full term	39 weeks	full term	ND	36 weeks	37 weeks	39 weeks
Birth length (cm)	ND	ND	36	ND	43.1	42	43	(average)	ND	44	44	44
Birth weight (g)	ND	2,200	2,124	2,832	2,535	2,222	2,485	3,500	ND	2,097	2,790	3,300
Clinical Features												
Height (cm) (SD)[a]	127.7 (−7.4)	130 (−7.0)	88.8 (−10.7)	94 (−4.0)	90 (−4.0)	118.4 (−5.1)	78.2 (−4.0)	118 (−9.1)	66 (−1.6)	90 (−6.8)	45 (−3.7)	81 (−5.9)
Weight (kg) (SD)[a]	40.3 (−2.2)	36.9 (−2.5)	13.2 (−3.7)	15.4 (−1.5)	14.4 (−1.3)	23.2 (−2.0)	10.6 (−1.9)	28 (−3.3)	5.65 (−3.0)	13.9 (−2.2)	2.65 (−2.8)	8.5 (−8.4)
Craniofacial												
Flat face with prominent forehead	ND	ND	+	+	+	+	+	−	+	+	+	+
Prominent eyes, proptosis	ND	ND	+	−	−	+	+	−	+	+	+	+
Blue sclerae	ND	ND	+	+	+	−	+	−	+	+	+	−
Long upper lip	ND	ND	−	+	+	−	+	+	+	+	+	−
Micrognathia	ND	ND	+	+	+	+	−	+	−	−	−	−
Cleft palate	ND	ND	−	−	−	−	−	−	−	−	−	+
Musculoskeletal												
Kyphoscoliosis[b]	+ (7 months)	+ (1.2 years)	+ (8 months)	+ (infancy)	+ (2 years)	+ (3 months)	+ (8 months)	+ (1 year)	+ (6 months)	++ (prenatal)	++ (prenatal)	++ (2 years)
Spatulate finger	−	ND	+	+	+	+	−	−	+	+	+	−
Finger laxity	ND	ND	+	+	−	−	+	−	++	+	+	+
Large joint laxity	ND	ND	+	+	−	−	+	−	++	++	++	+
Restricted elbow movement	+	ND	+	+	+	−	−	+	+	+	+	+
Hand contracture	−	−	−	−	−	+	−	−	−	+	+	−

(*Continued on next page*)